Arch. Mech., 48, 1, pp. 89–109, Warszawa 1996

Biaxial creep study of copper on the basis of isochronous creep surfaces

Z.L. KOWALEWSKI (WARSZAWA)

A METHODOLOGY for determination of isochronous creep rupture surfaces is proposed on the basis of creep investigations carried out on pure copper under complex stress state at 523 K. This procedure is also used to determine the curves of the same time to reach the minimum creep rate and curves representing the same time to tertiary creep period. Analysis of these curves shows that for the stress level taken into account as a reference point in the plane $(\sigma_{11}, \sqrt{3}\sigma_{12})$, the material damage degree increases proportionally until rupture is achieved. It means practically that such isochronous curves coincide. Verification of the selected fundamental creep rupture criteria is carried out on the basis of the experimental data. It is shown that the Sdobyrev creep rupture criterion gives the most suitable tool to describe the degradation process of copper subjected to long-term constant loading conditions at elevated temperature.

1. Introduction

IN STRUCTURAL COMPONENTS subjected to long-term constant loading, which corresponds to the creep conditions, the material damage process develops. Two essential periods of such a process can be distinguished. During the first one, the damage process develops without microscopically visible cracks due to the nucleation process and growth of the microvoids. At the end of this stage, the macroscopically observed crack appears in the form of one or several fissures. In the second stage of the rupture process, the dominant fissure propagates reducing, as a consequence, the admissible loading capacity of a construction element and leading finally to its failure. In most cases the duration of the second stage of damage process is negligibly short in comparison to the exploitation time of an element [1]. Experiments concerning the processes of microcrack nucleation and growth, which are responsible for the failure of materials during creep, show that failure mechanisms can be divided into the three following types [2–7]:

1. Brittle failure mechanism, in which the microdefects are created and developed on the grain boundaries perpendicular to the maximum principal tensile stress.

2. Ductile failure mechanism, in which the microdefects are created at the grain boundaries, and they are developing due to grain boundary slides.

3. Mixed failure mechanism being a combination of the simultaneously developing mechanisms mentioned above.

The rupture character and time to rupture depends mainly on the material and the type and level of loading. Brittle failure mechanism is dominant in the case of polycrystalline materials tested at low levels of the uni-axial stress states. Material degradation during this mechanism has an intergranular character. At high stress levels the rupture takes place mainly due to the ductile failure mechanism, for

which the damages have a transgranular character and develop due to the slides passing through the grains. All mechanisms mentioned above may influence the form of a failure criterion determining time to rupture. In the paper it is one of the issues discussed in detail.

However, the main goal of the paper is to present a methodology of determination of the same time-to-rupture surfaces on the basis of creep tests carried out on pure copper under plane stress state at elevated temperature. It is proposed to adopt this technique to determine the surface of the same time to obtain the minimum creep rate (also called the surface of the same duration of primary creep) and surfaces of the same time to tertiary creep period.

2. Phenomenological creep rupture equations

At stress levels lower than the yield limit of a material subjected to creep, KACHANOV [8] has proposed to ignore the current necking of a specimen and to assume that the load is carried only by the effective part of the specimen cross-section, being the difference between the initial cross-section and the damage area, i.e. the area being the sum of all voids or fissures areas. He has introduced a scalar measure of damage in the form of the parameter of cross-section continuity which is 1 at the beginning of the deformation process and 0 at a localized failure of the material. It can be expressed by

$$\psi = \frac{A}{A_0}, \qquad 1 \geq \psi \geq 0, \tag{1}$$

where A denotes the effective area of specimen cross-section, and A_0 denotes the initial area of the cross-section.

Instead of this parameter it is more convenient to use a damage measure being the parameter complementary to that proposed by Kachanov. Such parameter represents the Rabotnov damage measure [9] and it can be given by

$$\omega = 1 - \psi = \frac{A_0 - A}{A_0}, \qquad 0 \leq \omega \leq 1. \tag{2}$$

It can be physically interpreted as the area of all defects referred to the undamaged initial cross-sectional area. Using this parameter, RABOTNOV [9] proposed modifications of the constitutive equations suggested by KACHANOV [8]. For uniaxial tensile stress tests, the strain rate and damage evolution equations are assumed to have the following simple normalised form:

$$\begin{aligned} \frac{\dot{\varepsilon}}{\dot{\varepsilon}_0} &= \frac{1}{(1-\omega)^m}\left(\frac{\sigma}{\sigma_0}\right)^n, \\ \frac{\dot{\omega}}{\dot{\omega}_0} &= \frac{1}{(1-\omega)^\eta}\left(\frac{\sigma}{\sigma_0}\right)^\nu, \end{aligned} \tag{3}$$

where n, m, ν, η, $\dot{\varepsilon}_0$, $\dot{\omega}_0$, σ_0 are material constants.

At the beginning of the test, when the material is undamaged, the strain rate equation in set (3) reduces to Norton's law describing the steady creep rate, given by

$$\frac{\dot{\varepsilon}}{\dot{\varepsilon}_0} = \left(\frac{\sigma}{\sigma_0}\right)^n. \tag{4}$$

For constant stress level it is easy to integrate the equations in set (3) to obtain the time variations of strain and damage. By applying the rupture condition $\omega = 1$, it is possible to determine time to rupture t_R. Taking into account these conditions, the following relations [11] are obtained:

$$\begin{aligned}
\frac{\varepsilon}{\varepsilon_0} &= \lambda\left[1 - \{1 - (t/t_R)\}^{1/\lambda}\right], \\
\omega &= 1 - (1 - t/t_R)^{1/(\eta+1)}, \\
t_R &= \frac{1}{(\eta+1)\dot{\omega}_0(\sigma/\sigma_0)^\nu}, \\
\varepsilon &= \dot{\varepsilon}_0(\sigma/\sigma_0)^n t_R = \frac{\dot{\varepsilon}_0}{(\eta+1)\dot{\omega}_0}\left(\frac{\sigma}{\sigma_0}\right)^{n-\nu}, \\
\lambda &= (\eta+1)(\eta+1-m).
\end{aligned} \tag{5}$$

The creep theory proposed by Kachanov and Rabotnov was an inspiration to develop many new damage models, and it is considered as the beginning of the Continuum Damage Mechanics. Since it described only uni-axial creep behaviour, LECKIE and HAYHURST [11] have attempted to generalize the simple Rabotnov-Kachanov equations to multiaxial states of stress. The generalisation of Eqs. (3) to multiaxial stresses has been achieved by making the assumption that the influence of continuum damage on the deformation rate process is of a scalar character, and by the introduction of the homogeneous stress function which reflects the stress state effects on the time to rupture. The form of the generalisations was also influenced by the experimental results of JOHNSON *et al.* [12, 13] according to which the strain rates depend on the effective stress, and the components of strain rate tensor are proportional to the components of deviatoric stress. Leckie and Hayhurst also respected the fact, known from Johnson's tests, that when deterioration is taking place in the tertiary region, the ratio of the strain rate components remains practically constant and equals the value achieved in the steady state portion. Equations (3) can then be written as:

$$\begin{aligned}
\frac{\dot{\varepsilon}_{ij}}{\dot{\varepsilon}_0} &= \frac{3}{2}\left(\frac{\sigma_e}{\sigma_0}\right)^{n-1}\left(\frac{S_{ij}}{\sigma_0}\right)\left(\frac{1}{(1-\omega)^\mu}\right), \\
\frac{\dot{\omega}}{\dot{\omega}_0} &= \Delta^\nu \frac{1}{(1+\eta)(1-\omega)^\eta},
\end{aligned} \tag{6}$$

where $\Delta = \Delta(\sigma_{ij}/\sigma_0) = \sigma_{\max}/\sigma_0$ for copper, and $\Delta = \Delta(\sigma_{ij}/\sigma_0) = \sigma_e/\sigma_0$ for aluminium alloys. Integration of the damage evolution equation $(6)_2$ for the following boundary conditions: $\omega = 0$, $t = 0$ and $\omega = 1$, $t = t_R$, yields, after normalisation, the relation describing time to rupture in the form

$$\frac{t_R}{t_0} = \frac{1}{\Delta^\nu}. \tag{7}$$

Substitution of $t_R = t_0$ in (7) gives the equation of isochronous surface.

As mentioned above, the experimental results of JOHNSON *et al.* [12, 13] had an important role in developing new constitutive creep models, since they had carried out wide investigations for several different metals under complex stress states. They tried to find a correlation between time to rupture and such stress state parameters as:

1) maximum principal stress $\sigma_{\max}$, which controls the damage according to the Galileo hypothesis,

2) effective stress σ_e, which controls the damage according to the Huber – Mises criterion,

3) first invariant of the stress tensor J_1.

They have shown that the dependence of the rupture time upon the nature of the applied stress system for an aluminium alloy can be described by the octahedral shear stress criterion, whereas for pure copper – by the maximum principal stress criterion.

It has been found convenient to present the rupture results in terms of an isochronous surface which is that curve connecting the stress states with the same rupture times. For the plane stress conditions the isochronous surfaces obtained for different rupture criteria are illustrated in Fig. 1. According to JOHNSON [12, 13], the rupture criteria for aluminium alloy and pure copper represent the extremes of material behaviour, since the isochronous surface for many metals lies somewhere between these criteria. In spite of the fact that these observations have been made on the basis of a relatively limited amount of experimental data, and in certain cases they did not give precise description of rupture, they are still influencing the process of developing new creep damage models. Typical examples of such situation are: the rupture criterion applied by DYSON and MCLEAN [14] in which they assumed that the creep damage of Nimonic 80A tested at 1023 K was governed by the criterion being a product of the effective stress and maximum principal stress criteria, and the creep rupture criterion proposed by SDOBYREV [15] in the following form:

$$t_R^{(\mathrm{Sdob})} = A\{\beta\sigma_{\max} + (1-\beta)\sigma_e\}^{-\nu}, \tag{8}$$

where σ_e represents the effective stress defined by the second invariant of the stress deviator, $\sigma_{\max}$ denotes the maximum principal stress, β denotes the experimentally determined coefficient reflecting the relation between time to rupture and σ_e, $\sigma_{\max}$.

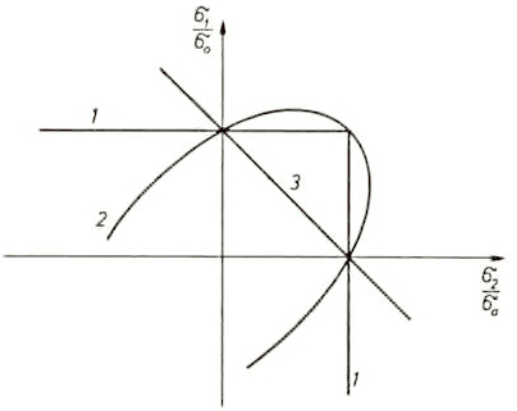

FIG. 1. Graphical representation of the creep rupture criteria (*1* – maximum principal stress criterion, *2* – Huber–Mises effective stress criterion, *3* – hydrostatic loading criterion).

On the basis of the experimental results obtained from tests made on cruciform specimens [2] and Johnson's investigations [12, 13], who used thin-walled tubular testpieces, HAYHURST [2], in attempts to describe the multi-axial behaviour of several materials, suggested a general relationship

$$t_R^{(\mathrm{Hay1})} = f(J_1, J_2, J_3), \tag{9}$$

where f is a homogeneous algebraic function of stress invariants. It has been found that both the relationships given by Eqs. (8) and (9) can be used to represent accurately the behaviour of copper alloys in the tension-compression quadrant of the diagram in Fig. 1, but predictions of the rupture time are in error for bi-axial tensile stresses. The bi-axial tension stress levels predicted by Eqs. (8) and (9) are too high and too low, respectively. On the basis of these remarks, HAYHURST [2] proposed a criterion which is capable of expressing the different types of behaviour represented by Eqs. (8) and (9) in the form

$$t_R^{(\mathrm{Hay2})} = A\left\{a\sigma_{\max} + bJ_1 + cJ_2'^{\frac{1}{2}}\right\}^{-\nu}, \tag{10}$$

being a linear combination of the maximum principal tensile stress and the first and second stress invariants; here A, ν – material constants which are independent of stress; a, b, c – constants; and J_1, J_2' represent the first invariant of the stress tensor and the second invariant of the stress deviator, respectively, which in terms of principal stresses are given by

$$\begin{aligned} J_1 &= \sigma_1 + \sigma_2 + \sigma_3\,, \\ J_2' &= \frac{1}{6}\left[(\sigma_1 - \sigma_2)^2 + (\sigma_2 - \sigma_3)^2 + (\sigma_3 - \sigma_1)^2\right]. \end{aligned} \tag{11}$$

In expression (10) a, b, c are constants with $a + b + c = 1$, what limits the influence of particular terms in the criterion (10) on the time to rupture. By selecting appropriate values of these constants, all the simple rupture criteria previously discussed can be represented, i.e.

I) the maximum principal stress rupture criterion, if $a = 1$, $b = c = 0$; its graphical interpretation for the biaxial stress state is represented by the two straight lines (*1*), Fig. 1;

II) the Huber–Mises effective stress criterion, if $c = 1$, $a = b = 0$, represented by the ellipse (*2*) in Fig. 1;

III) the maximum hydrostatic stress criterion defined by the first invariant of the stress tensor; if $b = 1$, $a = c = 0$, it is represented by the straight line (*3*) in Fig. 1.

3. Programme of investigations

3.1. Material, specimen and testing device

The material investigated was electrolytic copper (M1E) of 99.9% purity. It was annealed for two hours at 673 K and furnace-cooled to achieve a uniform grain size, and next it was aged at constant room temperature for five years. Creep investigations were carried out on thin-walled tubular testpieces shown in Fig. 2 with the use of the biaxial creep testing machine, enabling satisfaction of the plane stress conditions by simultaneous loading of the testpieces by an axial force and twisting moment at elevated temperature (523 K). Details of the

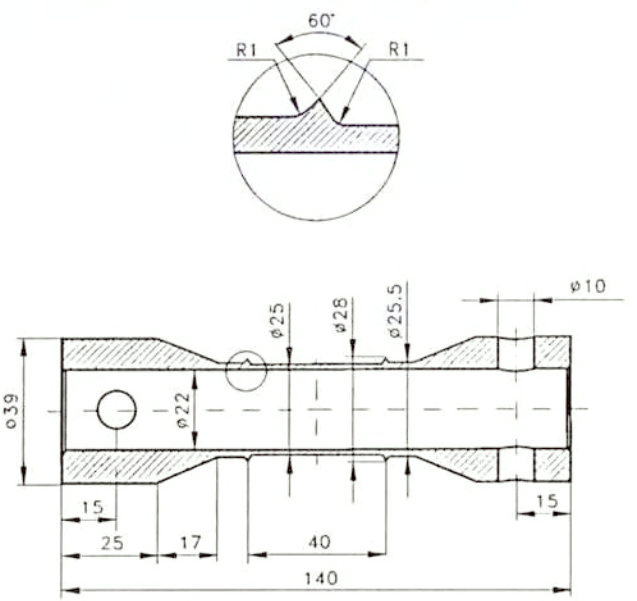

FIG. 2. Engineering drawing of the specimen.

experimental device are presented in [16, 17], whereas information concerning the measurement technique applied may be found in [18].

3.2. Experimental procedure

The experimental programme contained the creep tests up to rupture for copper specimens subjected to biaxial stress state, obtained by various combinations of an axial force and twisting moment leading to three different values of effective stress (σ_e = 70.0; 72.5; 75.0 [MPa]) defined by the following relationship:

$$\sigma_e = \left(\frac{3}{2} S_{ij} S_{ij}\right)^{1/2} = (\sigma_{11}^2 + 3\sigma_{12}^2)^{1/2}, \tag{12}$$

where S_{ij} – stress deviator, σ_{11} – axial stress, σ_{12} – shear stress. Diagram of the experimental programme is shown in Fig. 3. Creep tests under tension, torsion and combination of these loadings were carried out. The complex stress states in

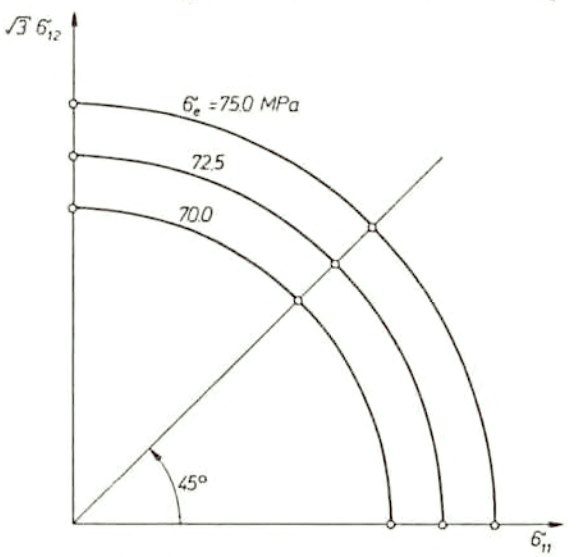

FIG. 3. Programme of creep tests.

the two-dimensional stress space (σ_{11}, $\sqrt{3}\sigma_{12}$) correspond to the points located on the rectilinear path of slope $\Theta_\sigma = 45°$ with respect to the σ_{11} stress axis. The angle Θ_σ was determined from the relation

$$\Theta_\sigma = \arctan\left(\frac{\sqrt{3}\sigma_{12}}{\sigma_{11}}\right). \tag{13}$$

Prior to creep test, each specimen was heated uniformly at the test temperature (523 K) for 24 hours. Creep investigations were carried out until rupture of the testpieces was achieved giving, as a consequence, the whole creep characteristics.

All creep tests were performed at stress levels which were lower than the value of yield point of the material at 523 K ($R_{0.2}$ = 76 [MPa]). Thus, the total strain has been expressed as a sum of the elastic and creep strain components in the form:

$$\varepsilon_{ij} = \varepsilon_{ij}^{(e)} + \varepsilon_{ij}^{(c)}, \tag{14}$$

where strain components with the superscripts e and c denote elastic and creep strain, respectively.

4. Creep tests results of copper

The creep curves up to rupture for copper are presented in Figs. 4, 5, 6 for uni-axial tension, combination of tension and torsion, and pure torsion, respectively. The horizontal axes in Figs. 4, 5, 6 correspond to the time, while the vertical ones correspond to the effective creep strain defined by the relation in the following form:

$$\varepsilon_e^{(c)} = \left(\frac{2}{3}\varepsilon_{ij}^{(c)}\varepsilon_{ij}^{(c)}\right)^{1/2} = \sqrt{\varepsilon_{11}^2 + \left(\frac{4}{3}\right)\varepsilon_{12}^2}, \tag{15}$$

where ε_{11} and ε_{12} denote axial and shear strain, respectively.

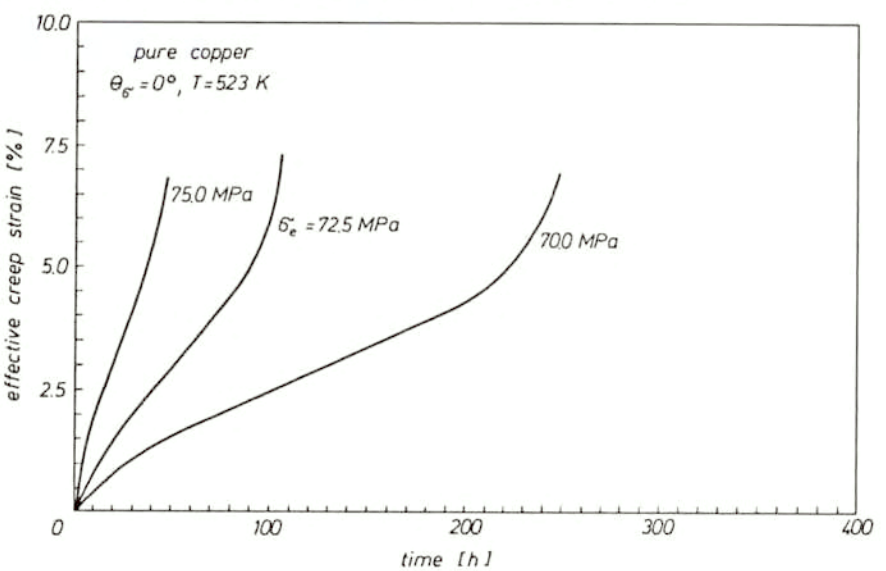

FIG. 4. Creep curves for copper tested under uni-axial tension.

The creep characteristics obtained at the same effective stress but under different stress states exhibit drastic differences for all the stress levels considered.

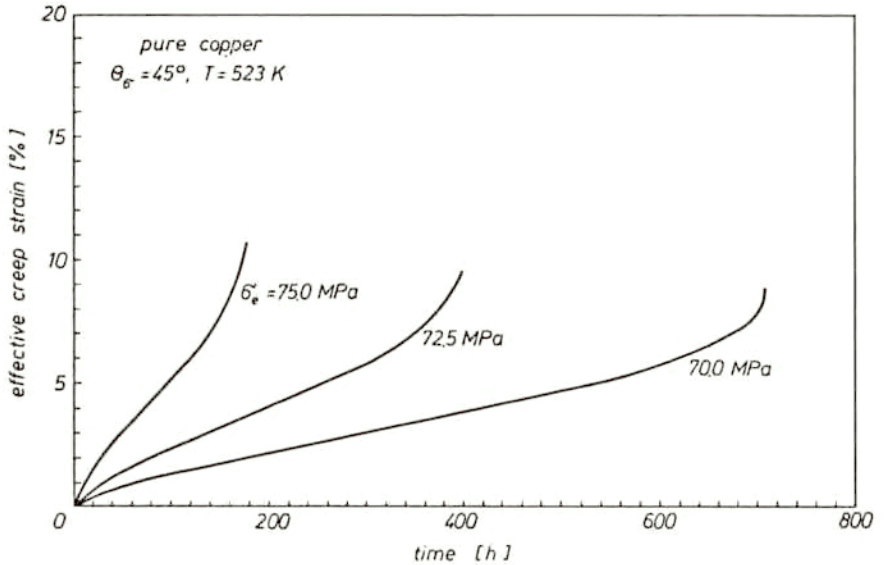

FIG. 5. Creep curves for copper tested under combination of uni-axial tension and pure torsion.

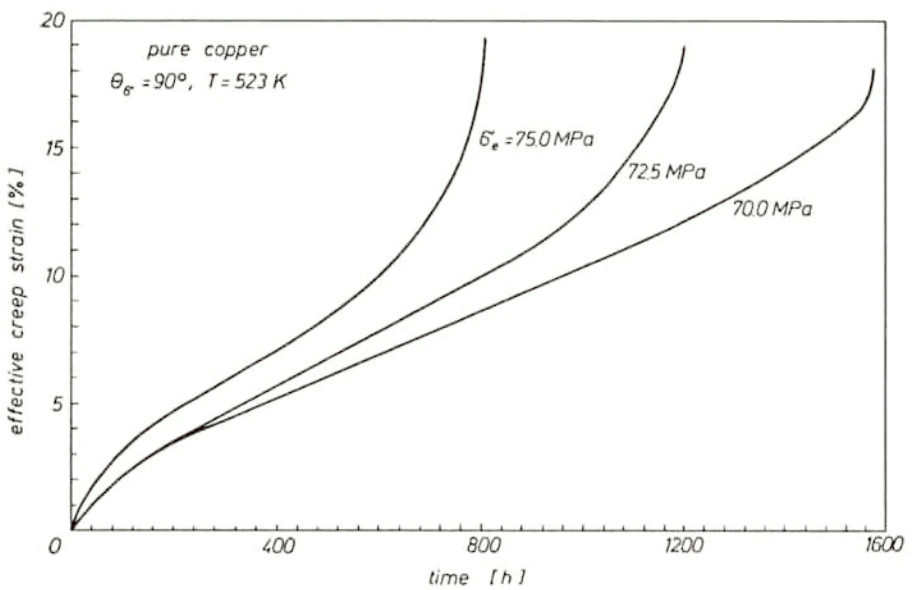

FIG. 6. Creep curves for copper tested under pure torsion.

In all cases the shortest lifetimes and, moreover, the lowest ductility have been achieved for tensioned testpieces. The opposite effect was observed for testpieces subjected to pure torsion. It has to be emphasized that differences in creep curves due to different loading types applied are considerable, and they are reflected by

variations of the basic creep parameters. All of them have been discussed in detail elsewhere [19]. In this paper they are only synthetically summarized in Table 1.

Table 1. Creep tests results for copper.

	σ_e = 70.0 [MPa]			σ_e = 72.5 [MPa]			σ_e = 75.0 [MPa]		
	$\Theta_\sigma=0°$	$\Theta_\sigma=45°$	$\Theta_\sigma=90°$	$\Theta_\sigma=0°$	$\Theta_\sigma=45°$	$\Theta_\sigma=90°$	$\Theta_\sigma=0°$	$\Theta_\sigma=45°$	$\Theta_\sigma=90°$
$\dot{\varepsilon}_e^{(c)}\times10^{-5}$ [1/h]	18.4	8.5	8.0	51.0	16.6	10.2	105.0	41.2	13.0
$\dot{\varepsilon}_{11}\times10^{-5}$ [1/h]	18.4	6.1	–	51.0	12.7	–	105.0	31.0	–
$2\dot{\varepsilon}_{12}\times10^{-5}$ [1/h]	–	10.2	13.9	–	18.5	17.7	–	47.0	22.5
t_R [h]	254	700	1560	101	391	1187	47	175	799
t_I [h]	50	90	260	25	65	200	15	45	160
t_{II} [h]	170	480	1000	70	255	760	35	125	450
$\varepsilon_e^{(c)}$ [%]	6.8	8.6	17.5	7.3	9.3	18.1	6.7	10.6	19.0

Notations in the Table 1: $\dot{\varepsilon}_e^{(c)}$ – minimum effective creep strain rate, $\dot{\varepsilon}_{11}$ – minimum axial creep strain rate, $\dot{\varepsilon}_{12}$ – minimum shear creep strain rate, t_R – time to rupture, t_I – duration of primary creep period, t_{II} – time to tertiary creep, $\varepsilon_e^{(c)}$ – effective creep strain at rupture.

5. Experimental data analysis

All the creep parameters, given in Table 1, which characterise macroscopically the creep behaviour prove that the process is stress-state-sensitive, in spite of the initial isotropy of the material in the sense of such parameters as Young's modulus, yield limit or ultimate tensile stress. Such material behaviour can be interpreted, on the one hand, as the material deformation due to different deformation mechanisms, activation of which is connected with the stress state type; on the other hand, however, it is known [2, 3, 14] that the majority of microcracks appearing at the grain boundaries are observed at those grain boundaries which are perpendicular to the maximum principal stress. It seems that for copper, the last conclusion can be confirmed by the shapes of the specimen cross-section in places where rupture has occurred. In case of creep tension tests the failure line was perpendicular to the main specimen axis, in case of complex stress states this line was inclined at angles equal typically to 15 – 20°, measured with respect to the line perpendicular to the main specimen axis, whereas for testpieces subjected to pure torsion these angles were approximately equal to 30 – 45°, Fig. 7. Thus, it can be concluded that for copper, the basic deformation mechanism seems to be the same for all stress state types considered, while the resulting variations in lifetimes for the same effective stress follow from the differences in the value of the maximum principal stress.

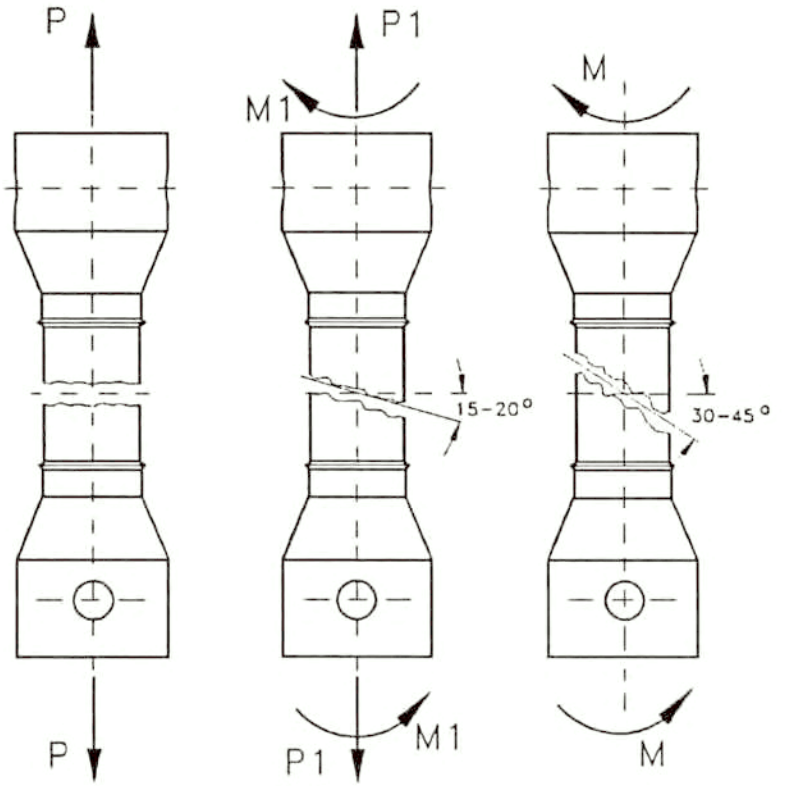

FIG. 7. Variations of the specimen failure line during creep at different types of stress states.

Clear presentation and comparison of the experimental data obtained from tests performed at complex stress states produce many difficulties, particularly for stress states being a combination of tension and torsion. In these cases, a comparison of results is usually carried out for the effective strains defined in the form of a function of the second invariant of the strain tensor, since the effects of the first as well as the third invariants are relatively small and they can be often neglected. Although creep curves in diagrams representing effective strains versus time can be compared, it is difficult to evaluate precisely all differences in material response due to the action of different stress state types. To overcome this deficiency, creep rupture results are commonly presented in the form of isochronous surfaces [1, 2, 11, 20–24], which in the stress space correspond to the same time to rupture. Experimental determination of the isochronous surface requires many creep tests at various stress states and at several stress levels. In the case of material anisotropy, there is practically no possibility to determine experimentally such a surface with sufficient accuracy. However, it can be done with a relatively good approximation on the basis of the relationship $\log(\sigma_e) = f[\log(t_R)]$, Fig. 8. In this figure results for the three types of stress states are presented. Data points

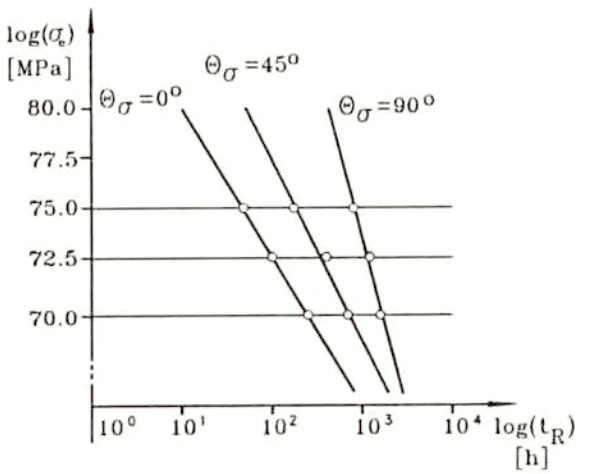

FIG. 8. Logarithmic diagram of the relation between effective stress and time to creep rupture for all stress states considered.

for the chosen type of stress state (with a relatively high accuracy) are located on the straight lines which have different mutual positions. These lines have been obtained by means of the least squares technique. Taking, as a reference point, the line representing pure torsion results, the remaining straight lines are shifted and rotated. Analysis of the mutual position of these lines indicates that the material subjected to creep process under uni-axial tension is significantly more sensitive to the stress variations, in comparison to the same material tested either at pure torsion or a combination of tension and torsion. On the basis of the diagrams shown in Fig. 8, drawing straight lines which are parallel to the stress axis and intersect the approximation lines representing the experimental data, it is easy to determine the points connecting the same times to rupture. The points for the rupture time taken into account provide the values of effective stresses necessary to achieve the rupture at the particular type of stress state considered. These values can be approximated on the stress plane $(\sigma_{11}, \sqrt{3}\sigma_{12})$ giving, as a consequence, the isochronous curves. Surfaces of the same lifetime determined in this way are shown in Fig. 9 for the rupture times equal to 200; 400, and 1000 [h]. It can be seen that the isochronous locus corresponding to the rupture time of 200 [h] is obtained for stress levels which are greater than those applied in experiments. Thus, a question arises in what range the relationship $\log(\sigma_e) = f[\log(t_R)]$ can be approximated by the straight lines for all stress types considered in the experimental programme. From the preliminary uniaxial tension creep tests made on copper it was known that in a logarithmic scale, the stress level was a linear function of lifetime in the limits considered, i.e. 60 – 90 [MPa]. Since the same behaviour has been also observed for this material by other researchers, e.g. ABO EL ATA and FINNIE [5], HAYHURST [3], in much wider stress limits and, moreover, taking into account the linearity of the relationship $\log(\sigma_e) = f[\log(t_R)]$ observed

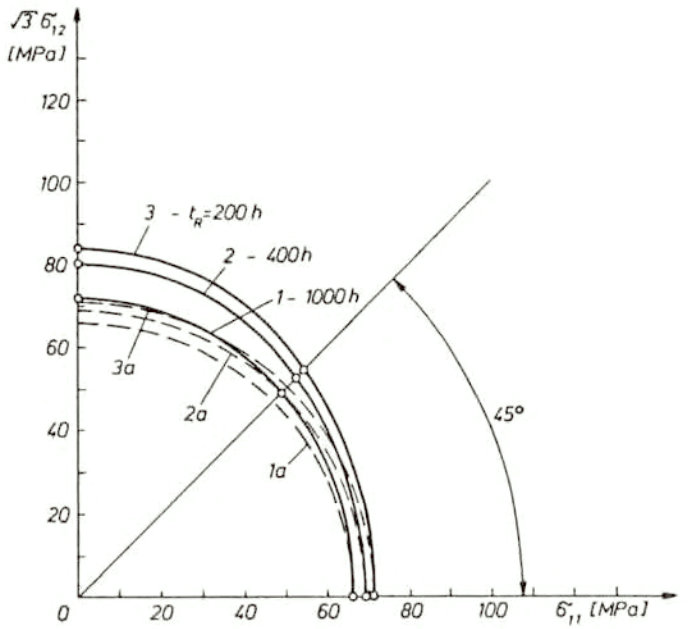

FIG. 9. Comparison of the isochronous creep rupture surfaces, t_R = 200; 400; 1000 [h], determined on the basis of experimental results (continuous lines) with the theoretical surfaces calculated for the Huber–Mises effective stress rupture criterion (dashed lines).

for the remaining loading cases ($\Theta_\sigma = 45°$, $\Theta_\sigma = 90°$) at stress levels within the range of 70 – 75 [MPa], it seems to be reasonable to extrapolate linearly this relationship for these loading combinations within the wider range representing ±20% of the average stress level applied in biaxial creep experiments.

The surface corresponding to the rupture time equal 400 [h] has been selected for further comparative studies on the isochronous surfaces predicted by the commonly used creep rupture criteria. Results of these considerations are presented in Sec. 6.

6. Verification of the fundamental creep rupture hypotheses

Applicability of the creep rupture criteria most frequently used is studied for the experimentally examined pure cooper. The curves of the same time to rupture, determined on the basis of the experimental programme realized, are compared with theoretical predictions of the following creep rupture hypotheses:

• the maximum principal stress rupture criterion, which is defined in the stress coordinate system $(\sigma_{11}, \sigma_{12})$ corresponding to the experimental programme by the following relationship

$$\sigma_R = \sigma_{\max} = \frac{1}{2}\left(\sigma_{11} + \sqrt{\sigma_{11}^2 + 4\sigma_{12}^2}\right), \tag{16}$$

• the Huber-Mises effective stress rupture criterion which, for the combinations of stresses used in experiments, takes the form

$$\sigma_R = \sigma_e = \sqrt{\sigma_{11}^2 + 3\sigma_{12}^2}\,, \tag{17}$$

• the Sdobyrev creep rupture criterion (8), which will be used in further considerations in the form

$$\sigma_R = \beta\sigma_{\max} + (1-\beta)\sigma_e\,. \tag{18}$$

The isochronous surfaces resulting from these rupture criteria are compared with the surface determined on the basis of experimental results in Fig. 10. All curves presented in the normalized coordinate system are referred to the rupture

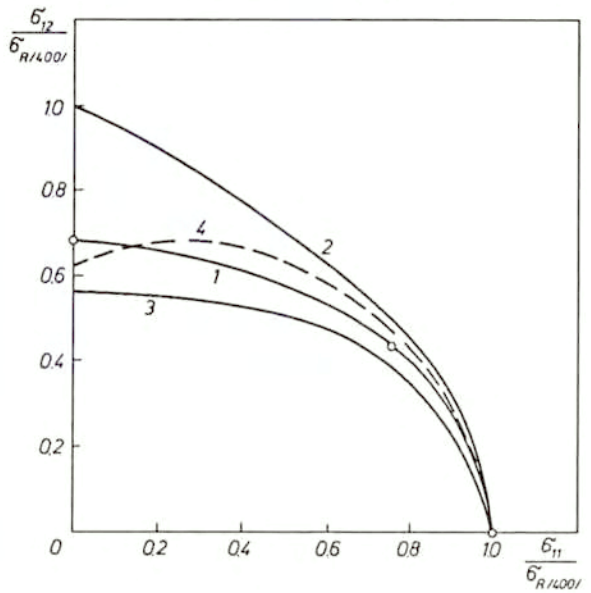

FIG. 10. Comparison of the isochronous creep rupture surfaces determined on the basis of experimental results (*1*) for t_R = 400 [h] with surfaces calculated according to: – the maximum principal stress rupture criterion (*2*), – the Huber–Mises effective stress rupture criterion (*3*), and – the Sdobyrev creep rupture criterion (*4*). Normalization of the coordinate system has been carried out with the use of the reference tension stress which gives the value of time to rupture 400 [h].

time equal to 400 [h]. Tensile stress corresponding to the lifetime of 400 [h] has been selected as the normalization value ($\sigma_{R/400/}$). As it is clearly seen, the best description of the experimental data has been achieved for the Sdobyrev creep rupture criterion taken with the coefficient β = 0.9, calculated on the basis of creep tests carried out. The value of β indicates that the damage mechanism governed by the maximum principal stress played a considerable role in the creep

rupture of the copper tested. Thus, this result can be treated as a confirmation of the earlier observed creep behaviour of copper having similar chemical composition [2, 3, 12, 13].

7. Method of determination of surfaces representing the same duration of primary creep and the same time to tertiary creep period

Typical creep process can be divided into three stages. In the first period the strain rate gradually decreases until minimum creep rate is achieved, the value of which is further maintained at the whole secondary creep stage. An increase of strain rate characterises the tertiary period of creep process, at the end of which rupture of the specimen tested occurs at time t_R. Such development of the phenomenon is connected with the increase of structure degradation velocity of a material which is manifested by the growth of voids and microcracks existing mainly at the grain boundaries. The material continuum is disturbed due to the microcracks propagation and due to development of other structural defects, what in consequence leads to the reduction of stiffness, and finally to rupture.

In the previous section it has been shown how to present clearly the experimental creep rupture results. Since the creep damage process already appears at the primary creep [25], it seems to be reasonable to adopt the isochronous surface concept at other characteristic points of the creep curve, such as the end of the primary or of secondary creep periods. Obviously, it is possible only if the conditions of the process and the material tested ensure the typical creep curve, i.e. a curve having all creep stages. In practice, the loading conditions and materials of structural components satisfy these conditions.

7.1. Isochronous curves of the end of primary creep period

Determination procedure of the curves representing the same duration of primary creep is analogous to that used to obtain surfaces of the same time to rupture. Thus, in the first step, the diagrams $\log(\sigma_e) = f[\log(t_1)]$ have been prepared for all stress states types considered in the plane $(\sigma_{11}, \sqrt{3}\sigma_{12})$. Similarly to the rupture times considerations, data points for the chosen type of stress state, with relatively high accuracy, are located on the straight lines which have different mutual positions, Fig. 11. These lines have been obtained by the least squares method. Taking as a reference point the line representing pure torsion results, the remaining straight lines are shifted and rotated. Analysis of the mutual location of these lines indicate that the material subjected to creep process under uni-axial tension is significantly more sensitive to the stress variations than the same material tested either at pure torsion or at a combination of tension and torsion. On the basis of diagrams shown in Fig. 11, it is easy to determine points connecting the same times to achieve stabilization of the creep strain rate. The points, for a chosen duration of primary creep period, provide values of effective

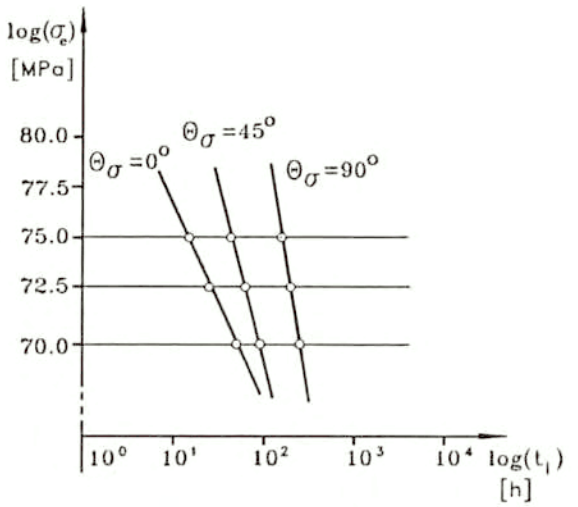

FIG. 11. Logarithmic diagram of the relation between effective stress and duration of primary creep for all stress states considered.

stresses necessary to achieve the end of primary creep at a particular type of the stress state considered. These values can be approximated on the stress plane $(\sigma_{11}, \sqrt{3}\sigma_{12})$ giving, as a consequence, the isochronous curves which describe the stress states corresponding to the end of primary creep. In Fig. 12 the surfaces of the same duration of primary creep period are shown for the time t_I equal to 50; 100, and 200 [h].

It can be seen that the shape and dimensions of the isochronous surfaces representing the same time to rupture (Fig. 9) and the same duration of primary creep period (Fig. 12) are similar. However, in order to compare them accurately it is necessary to provide clearly defined reference point. In order to assess mutual correlation of both types of isochronous surfaces, the tension stress equal 68.5 [MPa] has been selected as a reference point, which corresponds to the lifetime of 400 [h]. The cross-section of the isochronous surface for this rupture time is represented in Fig. 9 by the curve *2* and in Fig. 10 by the curve *1*. Taking into account the reference tension stress level and using diagrams $\log(\sigma_e) = f[\log(t_I)]$, shown in Fig. 11, it is easy to find the time to creep strain rate stabilization (t_I = 68 [h]). Knowing this value, all stress levels for the considered stress states which correspond to the same duration of primary creep can be determined, Fig. 11, giving the data necessary to obtain the isochronous surface. Comparison of the surfaces representing the same lifetime and the same duration of primary creep period is presented in Fig. 13. It is easy to see a great similarity of these surfaces. Thus, it can be stated for the tested copper that, on the basis of the degree of creep process development at the end of primary creep, represented by the surface of the same duration of primary creep, we can deduce the shape

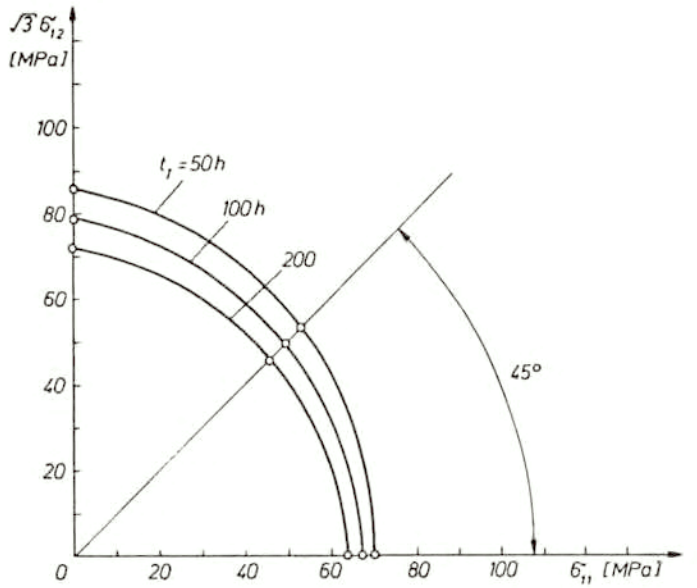

FIG. 12. Isochronous surfaces representing the same duration of primary creep period, t_1 = 50; 100; 200 [h], determined on the basis of experimental results.

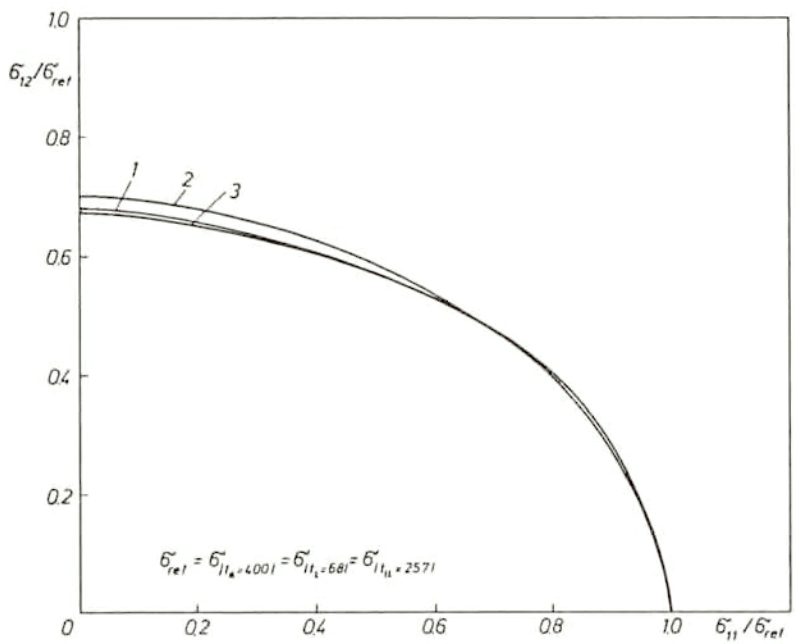

FIG. 13. Comparison of the experimentally determined surfaces representing the same time to rupture (*1*), the same duration of primary creep period (*2*), and the same time to tertiary creep period (*3*). The stress level at uni-axial tension which corresponds to: the time to rupture 400 [h], duration of primary creep 68 [h], and time to tertiary creep 257 [h] is used as a normalization factor.

of isochronous surface describing the same time to rupture. In other words, the degree of damage evolution in copper for each loading type in the experimental programme maintained a constant value.

In order to confirm this suggestion, the other characteristic point of the creep curve, i.e. time to tertiary creep, will be discussed in the next section.

7.2. Isochronous curves of the end of secondary creep period

The curves representing the same time to tertiary creep are determined by the same method as that used to obtain surfaces of the same time to rupture and the same duration of primary creep. First of all, the diagrams $\log(\sigma_e) = f[\log(t_{II})]$ have been prepared for all stress states types considered in the plane $(\sigma_{11}, \sqrt{3}\sigma_{12})$. Similarly to the rupture times considerations, data points for the chosen type of stress state are again located, with relatively high accuracy, on the straight lines which have different mutual positions, Fig. 14. As previously, these lines have been obtained by means of the least squares technique. On the basis of the diagrams

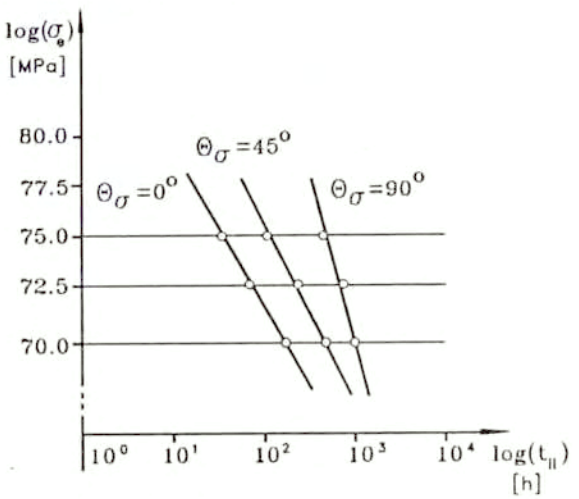

FIG. 14. Logarithmic diagram of the relation between effective stress and time to tertiary creep for all stress states considered.

shown in Fig. 14, the points connecting the points of the same times to tertiary creep can be determined. For the chosen time to tertiary creep period, these points provide the values of effective stresses necessary to achieve the end of secondary creep at a particular type of the stress state considered. These values can be approximated on the $(\sigma_{11}, \sqrt{3}\sigma_{12})$ stress plane, giving the isochronous curves which describe the stress states corresponding to the initiation of tertiary creep. In Fig. 15 the surfaces of the same time to tertiary creep period are shown for the time t_{II} equal to 100; 200, and 400 [h].

The shape and dimensions of the isochronous surfaces representing the same time to tertiary creep (Fig. 15), the same duration of primary creep period (Fig. 12),

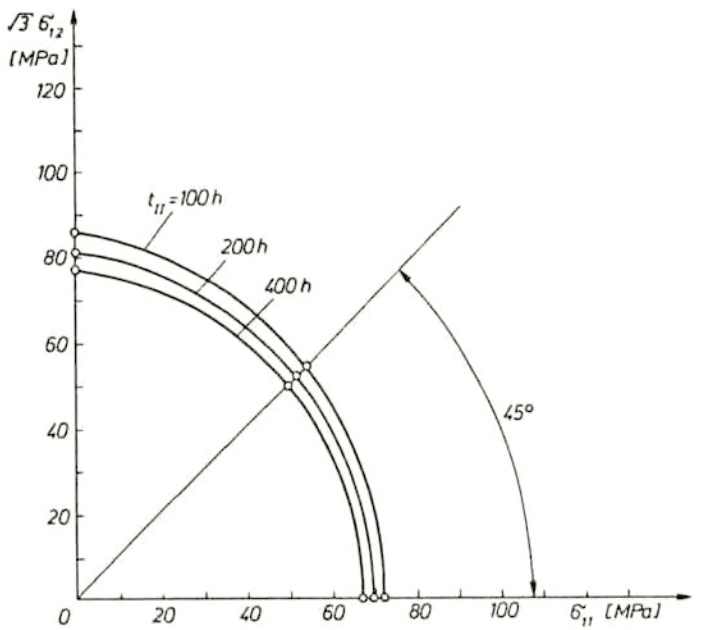

FIG. 15. Isochronous surfaces representing the same time to tertiary creep period, t_{II} = 100; 200; 400 [h], determined on the basis of experimental results.

and the same time to rupture are similar. However, in order to compare them, it is necessary to provide clearly defined reference point, selected in the same manner as in the previous section. Taking into account the tension stress level (68.5 [MPa]) as the reference point and using diagrams $\log(\sigma_e) = f[\log(t_{II})]$ shown in Fig. 14, it is easy to find the time to tertiary creep period (t_{II} = 257 [h]). Knowing this value, all stress levels corresponding to the same time to tertiary creep can be determined for the types of stress states considered, Fig. 14. It gives the data necessary to obtain the isochronous surface which reflects the same time to tertiary creep in the two-dimensional stress space $(\sigma_{11}, \sqrt{3}\sigma_{12})$. Comparison of the surfaces representing: (i) the same lifetimes; (ii) the same time to stabilization of the creep rate, and (iii) the same time to tertiary creep period, is presented in Fig. 13. It is easy to note that these surfaces are almost coincident. Such mutual location of the surfaces confirms the previously suggested thesis about the same degree of damage development in copper, measured as the ratio of the effective stress to the selected reference tension stress for the chosen direction in the $(\sigma_{11}, \sqrt{3}\sigma_{12})$ plane.

The knowledge of such material behaviour during creep makes it possible to simplify the procedure of determination of the isochronous creep rupture surfaces, since in such a case it is sufficient to carry out the creep tests with duration limited to the secondary creep period. Only one of them should be continued until rupture is achieved. On the basis of the isochronous surface

representing the same time to stabilization of a creep rate, and knowing the time to rupture for an arbitrary direction chosen in the $(\sigma_{11}, \sqrt{3}\sigma_{12})$ plane, it is easy to determine the isochronous creep rupture surface at the entire stress range considered.

8. Conclusions

The results of creep experiments made on pure copper under complex stress state at elevated temperature have been presented.

For the tested material such creep parameters analyzed as: duration of primary creep period, minimum creep rate, time to rupture and ductility were the functions of the type of stress state.

The procedure of determination of the isochronous creep rupture surfaces is proposed. In spite of the fact that this method can be applied to a limited range of stresses, i.e. stress levels close to those used in experiments, it gives a promising tool in multiaxial data analysis.

The procedure used to determine the isochronous creep rupture surfaces can be also applied to obtain both surfaces representing the same time to stabilized creep rate and surfaces of the same time to attain tertiary creep period. Analysis of all types of the isochronous surfaces for copper proved that the damage evolution develops proportionally until the creep rupture is achieved for different stress types taken into account in the $(\sigma_{11}, \sqrt{3}\sigma_{12})$ stress space.

The brittle failure was observed for copper under the considered testing conditions. Verification of the fundamental creep rupture criteria has shown that the Sdobyrev creep rupture criterion gives a promising tool to describe the damage process of the material subjected to the long-term constant loading conditions at elevated temperature. However, it was shown that the mechanisms depending on the maximum principal stress essentially influence creep rupture of the tested copper, what is in agreement with earlier observations.

References

1. S. PIECHNIK and M. CHRZANOWSKI, *Time of total creep rupture of a beam under combined tension bending*, Inst. J. Solids Struct., 6, 453–477, 1970.
2. D.R. HAYHURST, *Creep rupture under multi-axial states of stress*, J. Mech. Phys. Solids, **20**, 381–390, 1972.
3. D.R. HAYHURST, *On the role of creep continuum damage in structural mechanics*, [in:] Engineering Approaches to High Temperature Design, B. WILSHIRE, D.R.J. OWEN [Eds.], Pineridge Press, Swansea, 85–176, 1983.
4. B.F. DYSON and T.B. GIBBONS, *Tertiary creep in nickel-base superalloys: analysis of experimental data and theoretical synthesis*, Acta Metall., **35**, 9, 2355–2369, 1987.
5. M.M. ABO EL ATA and I. FINNIE, *On the prediction of creep-rupture life of components under multiaxial stress*, Proc. of IUTAM Symp. on "Creep in Structures 1970", Gothenburg, 80–95, Springer-Verlag, 1972.
6. R.J. BROWNE, D. LONSDALE and P.E.J. FLEWITT, *The role of stress state on the creep rupture of 1%Cr1/2%Mo and 12%Cr1%MoVW tube steels*, [in:] Creep and Fracture of Engineering Materials and Structures, Pineridge Press Ltd, Swansea, 545–557, 1981.

7. M.F. ASHBY, C. GANDHI and D.M.R. TAPLIN, *Fracture-mechanism maps and their construction for f.c.c. metals and alloys*, Acta Metallurgica, **27**, 699–729, 1979.
8. L.M. KACHANOV, *The theory of creep* [English translation edited by A.J. Kennedy], National Lending Library, Boston Spa 1958.
9. Y.N. RABOTNOV, *Creep problems in structural members*, North Holland Publishing Company, Amsterdam 1969.
10. F.H. NORTON, *Creep of steel at high temperatures*, McGrow-Hill, New York 1929.
11. F.A. LECKIE and D.R. HAYHURST, *Constitutive equations for creep rupture*, Acta Metallurgica, **25**, 1059–1070, 1977.
12. A.E. JOHNSON, J. HENDERSON and V.D. MATHUR, *Combined stress fracture of commercial copper at 250 C*, The Engineer, 202, 261, 1956.
13. A.E. JOHNSON, J. HENDERSON and B. KHAN, *Complex-stress creep, relaxation and fracture of metallic alloys*, H.M.S.O., Edinburgh 1962.
14. B.F. DYSON and D. MCLEAN, *Creep of Nimonic 80A in torsion and tension*, Metal Sci., **11**, 2, 37–45, 1977.
15. V.P. SDOBYREV, *Creep criterion for some high-temperature alloys in complex stress state* [in Russian], Izv. AN SSSR. Mekh. and Mashinostr., 6, 12–19, 1959.
16. Z. KOWALEWSKI, *The surface of constant rate of energy dissipation under creep and its experimental determination*, Arch. Mech., **39**, 445, 1987.
17. Z. KOWALEWSKI, *The influence of plastic anisotropy on the creep of metals under complex stress states* [in Polish], IFTR Reports 36, 1987.
18. W. TRĄMPCZYŃSKI and Z. KOWALEWSKI, *A tension-torsion testing technique*, Proc. Symp. "Techniques for Multiaxial Creep Testing", Elsevier Applied Science, London and New York, 79–92, 1986.
19. Z.L. KOWALEWSKI, *Experimental evaluation of the influence of stress state type on creep characteristics of copper at 523 K*, Arch. Mech., **47**, 1, 13–26, 1995.
20. M. CHRZANOWSKI and J. MADEJ, *The construction of failure limit curves by means of a damage* [in Polish], Theoretical and Applied Mech., **18**, 4, 587–601, 1980.
21. E. ROGALSKA, *Isochronous creep rupture curves*, Engng. Trans., **38**, 2, 295–306, 1990.
22. A. LITEWKA, *Creep rupture of metals under multi-axial state of stress*, Arch. Mech., **41**, 3–23, 1989.
23. A. LITEWKA and J. HULT, *One-parameter CDM model for creep rupture prediction*, Eur. J. Mech., A/Solids, **8**, 3, 185–200, 1989.
24. D.R. HAYHURST, W.A. TRĄMPCZYŃSKI and F.A. LECKIE, *Creep rupture under non-proportional loading*, Acta Metall., **28**, 1171–1183, 1980.
25. R.C. BOETTNER and W.D. ROBERTSON, *Study of growth of voids in copper during creep process by measurement of accompanying change in density*, Trans. Metall. Soc. A.I.M.E., **221**, 613, 1961.

POLISH ACADEMY OF SCIENCES
INSTITUTE OF FUNDAMENTAL TECHNOLOGICAL RESEARCH

Received February 27, 1995.